

Automobile Driving Interface Using Gesture Operations for Disabled People

Yoshitoshi Murata and Kazuhiro Yoshida
Faculty of Software and Information Science
Iwate Prefectural University
Takizawa, Japan

y-murata@iwate-pu.ac.jp, kyoshida@ipu-office.iwate-pu.ac.jp

Abstract— A steering operation interface has been designed for disabled people that uses right and left gesture operations. A questionnaire survey on gestures made with appendages had shown that gestures other than right and left ones were not suitable for driving a car. The interface incorporates both non-linear and semi-automatic steering control. Experiments using gyro sensors and a driving simulator demonstrated that driving operation using the foot, forefinger, wrist, or lower arm after training was close to conventional steering wheel operation. Sufficient practice in using the proposed interface should therefore enable users to achieve steering control close to that achieved with a steering wheel.

Keywords— automobile driving interface; disabled people; gyro sensor; gesture operation; appendage operation; driving simulator

I. INTRODUCTION

Disabled people generally want to stand on their own two feet, and achieving mobility is an important step in doing this. One way for them to enhance mobility is by driving automobiles to which driving-assistance devices have been attached. However, there has been a lack of development of new automobile driving interfaces that would enable disabled people, especially people with arm and wrist disabilities, to drive cars. Hence, we are designing a new steering operation interface for disabled people that is operated by gestures. We developed a prototype control device that used a gyro sensor, evaluated it by using a driving simulator and a skillful participant, and presented it at the Association for Community Health Improvement (ACHI 2013) [1].

The first auxiliary device for people with arm and wrist disabilities, the original of Honda's Franz system [2], was developed in the 1960s. A car is operated with only the feet in this system. Since the steering wheel is turned by pumping the pedals, its operation is not intuitive.

The autonomous car and the brain controlled car are ideal solutions for disabled people. Autonomous cars have been developed by many automobile manufacturers in addition to those by Google [3][4]. They need a very detailed 3D-map and many sensors to detect pedestrians, other cars, and obstacles around them. Therefore, their manufacturing costs must be expensive. Brain controlled cars have also been developed by researchers including those by automobile manufacturers [4][5]. A skillful driver for the brain control interface can indicate several kinds of commands. The

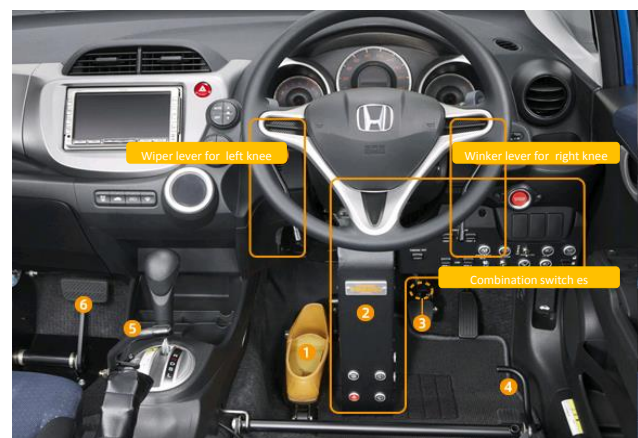
control is not accurate for letting the brain controlled cars operate within open traffic. Autonomous car technologies are needed for brain controlled cars to drive on usual roads. That is to say, brain controlled cars also need detailed 3D-maps and many sensors, and they are expensive. A current realistic solution for disabled people is to control steering with bodily appendages they can move.

The steering wheel in the system developed by Wada and Kameda was controlled with a joystick, and the brake and accelerator were controlled with another joystick [6][7]. This system has aided many disabled people, but strength is needed to operate the joysticks. Moreover, the levers onto which the joysticks were fixed had to be customized for the hand positions of individual users.

In any case, mechanical devices such as these lack flexibility and have to be customized for users. Hence, they are inherently expensive.

The on-going shift from hydraulic to electronic driving interface systems (e.g., steering and braking) means that systems combining computer chips with sensors can now be used to easily control these driving interfaces. Candidate sensors include Kinect sensors and gyro sensors.

In this paper, we verified the results we presented in ACHI 2013 by checking them in experiments, and investigated what movements by appendages drivers found to be natural by administering questionnaires.



(1) Steering pedal
(2) Steering box
(3) Brake lock button
(4) Selection bar for feet
(5) Side brake for knee
(6) Sub-brake for exercise

Figure 1. Honda's Franz system

After related work is discussed in Section II, we will describe the driving simulator we developed to evaluate our proposed driving interface in Section III. Gestures, i.e., movements by appendages assigned to various functions are explained in Section IV and the driving interface equipment we developed is presented in Section V. The experimental evaluation we conducted is described in Section VI. The key points are summarized and future work is mentioned in Section VII.

II. RELATED WORK

Since the purpose of this study is to design a steering operation interface for disabled people that is operated by gestures, we introduce an advanced driving interface for people who have difficulty moving their arms and/or hands. We also introduce sensors that support driving a car by gesturing.

A. Driving Interface for Disabled people

The Franz system used by Honda is aimed at people who have difficulty moving their arms and hands. The user operates a car with only his or her feet [2]. It was originally implemented in a Honda Civic in 1982, which was the first vehicle to introduce the Franz system in Japan. It has now been implemented in a Honda Fit.

The steering wheel is turned right or left by pumping a steering pedal (see Fig. 1). The transmission is shifted into drive by lifting the selection bar, into reverse by pushing it down, and into park by pushing it further down. The turn signals and windshield wipers are operated by turning levers with the right and left knees. Power windows and lights are controlled by flipping switches up or down with the right foot or knee.

Wada and Kameda developed a car driving interface for people who do not have enough strength to control a steering wheel, accelerator pedal, or brake pedal. They used joysticks instead of a steering wheel and pedals. Steering, braking, and acceleration in the initial version [5] were controlled with one joystick. Two joysticks are used in the latest version shown in Fig. 2 [6]. The joystick on the right controls the steering and that on the left controls acceleration and braking. The relationship between the angle of the steering wheel and the angle of the joystick is a polyline, as seen in Fig. 3. This means that a driver can sensitively control the steering wheel around a neutral position and can turn the wheel quickly when making a wide turn. People who can freely move their hands can drive automobiles with this device.

However, such mechanical devices must be customized to fit individual users' disabilities and physical form.

B. Sensors for gesturing

Several driving interfaces using Kinect sensors have been developed. A user can drive a virtual car in a simulated world with the "Air Driving" interface developed by Forum8 by moving his or her hands and feet in front of a sensor [8]. Since there must be at least 50 cm between the sensor and the appendage that is gesturing, it cannot be used in actual cars. Rahman et al. developed an interface for car audio operation that used a Kinect sensor [9]. Although this

interface has been demonstrated in an actual car, its use as a driving interface (e.g., steering and braking) has not been investigated.

Döring et al. developed a multi-touch steering wheel that could not only control steering but also the car audio [10]. However, users with arm disabilities had trouble operating it.

Other examples of using acceleration sensors and/or gyro sensors as gesture operation interfaces include those in video games and home appliance remote controls [11].

Unfortunately, there were not existing sensors for gesturing to control a steering wheel, accelerator pedal, and a brake pedal in an actual car.



Figure 2. Wada and Kameda's joystick driving interface

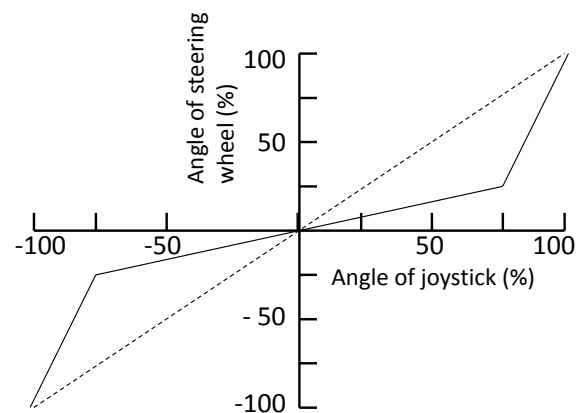


Figure 3. Relationship between angle of joystick and angle of steering wheel

III. DRIVING SIMULATOR

Before evaluating the proposed driving interface in an actual car, we evaluated it in a driving simulator to avoid traffic accidents. We introduce our developed driving simulator in this section.

A. Driving course

As one of our ultimate aims is to help disabled people obtaining a driver’s license, we design a driving simulator to not only measure driving operability, but also exercise when driving. The three main issues with the driving simulator are:

- (1) The feel of driving has to be similar to that of a real car.
- (2) It has to be possible to measure the position of the car within driving lanes.
- (3) It has to be easy to choose various driving courses from real roads.

We extract road data from maps such as Google Maps. The creation tools prepare 3D roads from extracted data, as shown in Fig. 4 [12]. We use OpenGL [13] as the 3D program interface and develop a program using the “glut”, “sdl” [14], “glew” [15], and “OpenAL” tools [16].

First, the simulation program has to find a direction perpendicular to the parametric curve that expresses the center line of the road to create the width of an approximated road, and it then calculates the coordinates of a point shifted to the right or left of the center line, as shown in Fig. 5.

A tangential angle of an arbitrary point on the curve can be calculated as

$$\theta = \text{Tan}^{-1} \frac{dy}{dx} \tag{1}$$

The point of the road edge is a position that shifts to the road width from an arbitrary point on the curve. The point of the road edge can be calculated as

$$\begin{aligned} x_r(t) &= W_r \cdot \cos(\theta - \frac{\pi}{2}) + x(t) \\ y_r(t) &= W_r \cdot \sin(\theta - \frac{\pi}{2}) + y(t) \\ x_l(t) &= W_l \cdot \cos(\theta + \frac{\pi}{2}) + x(t) \\ y_l(t) &= W_l \cdot \sin(\theta + \frac{\pi}{2}) + y(t) \end{aligned} \tag{2}$$

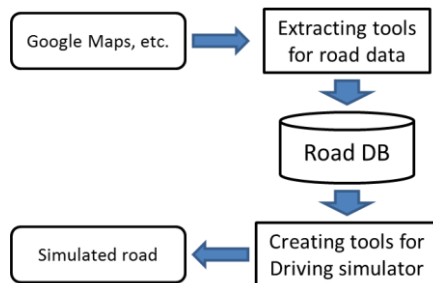


Figure 4. Outline for creating driving simulator road

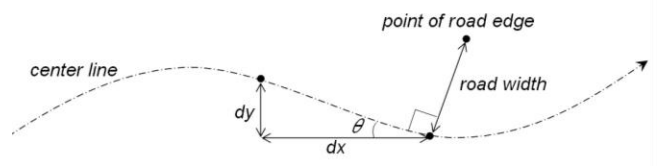


Figure 5. Method of creating 3D roads

3D road polygons are created by changing three-dimensional spline curve parameter “t” from zero to one, calculating many points on the road edge, and storing these points in a vertex array. Road center lines and lane lines are created by changing value W in Eq. (2).

When the width or the number of lanes at a curve’s parameter, $t = 0$, differs from the width or number of lanes at $t = 1$, the simulation program finds that the road has a right- or left-turn-only lane. When a road has a right- or left-turn-only lane, the road width has to be gradually increased. The simulation program in our system calculates a smooth curve that expresses increments in the width of the lane. We used the sigmoid function to increase the width. The sigmoid function is a monotonic increase function and has one inflection point. Therefore, it is suitable for expressing a right- or left-turn-only lane.

The polygon for a crossing consists of all curve functions that connect the crossing. The calculated curve function’s parameter “t” changes from zero to one in the same way as for a road, and a crossing polygon is created.

Fig. 6 has examples of a 3D road environment created by the simulation program according to this method.



(a) Example of straight road



(b) Example of crossing

Figure 6. Examples of created 3D roads

B. Motions of car

Two motions are simulated: gyration and acceleration [17][18].

1) Gyration

Steady gyrating motion is applied to the car under three main assumptions.

- The movement of the car is broadside motion of a rigid body. That is, the car is rigid and free of distortion.
- The speed is constant throughout each curve.
- The characteristics of the tires on the right are the same as those on the left.

The radius, R , of gyrating movement is given by the following equation, in which V is the running speed and δ is the steering angle.

$$R = (1 + CV^2) \frac{1}{\delta}. \quad (3)$$

The C is given by the following equation, in which the mass of the car is m , the cornering force on the front tires is K_f , that on the rear tires is K_r , the wheel base is l , and the distances between the car's center of gravity and the front and rear axles are l_f and l_r .

$$C = -\frac{m}{2l^2} \frac{l_f K_f - l_r K_r}{K_f K_r}. \quad (4)$$

Each parameter is set to produce driving characteristics similar to those of an actual car. The cornering force is controlled by adjusting the radius of the gyrating movement, i.e., the larger the radius, the stronger the cornering force.

2) Acceleration

The acceleration, A_c , of an actual car depends on the engine torque, the transmission gear ratio, the tire radius, the vehicle weight, and the engine speed. The engine speed depends on the degree to which the accelerator pedal is pressed.

Air resistance R_a and rolling resistance R_r are considered to be the total running resistance.

$$R_a = \frac{1}{2} C_d \rho S V^2, \quad (5)$$

where C_d is the aerodynamic coefficient, ρ is the fluid density of air, and S is the total surface area of the car.

$$R_r = C_{rr} m g, \quad (6)$$

where m is the mass of the car, C_{rr} is the rolling coefficient, and g is the gravitational acceleration. The resulting acceleration, A , is given by

$$A = A_c - (R_a + R_r). \quad (7)$$

C. Simulation display

There is an example view seen through the windshield in Fig. 7. The upper right shows the position of the car on the course. The operation monitoring tool we developed to facilitate operation is shown in Fig. 8. It helps the driver recognize the angle of the sensor from the angle of the steering wheel and the angle of the toes in case of rolling the ankle. It also displays the degree to which the accelerator or brake pedal has been pushed.



Figure 7. Example view through front window

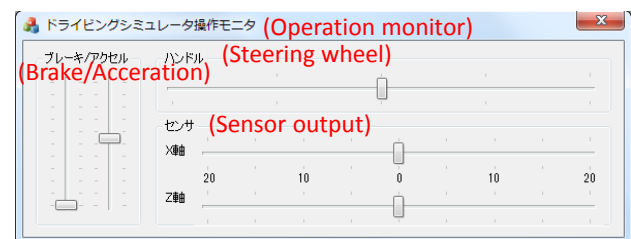


Figure 8. Operation monitoring tool

D. Measured data

Nine data items are measured.

- 1) Steering angle
- 2) Running speed
- 3) Distance driven and driving time
- 4) Position of car on course
- 5) Distance between left of car and left lane marker line
- 6) Distance between right of car and right lane marker line
- 7) Degree to which accelerator pedal was pushed
- 8) Depth to which brake pedal was pushed
- 9) Angle of car relative to driving direction

IV. GESTURES (MOVEMENTS BY APPENDAGES) FOR OPERATION

Here we describe the requirements for steering operation and control schemes that satisfy them. We then describe gestures for each body part on which a sensor is attached.

A. Operating functions

It is necessary to have door open/close, window open/close, wiper on/off, and turn signal on/off functions to drive an automobile in addition to the basic operations of steering, braking, and accelerating. Moreover, since automobiles typically have an audio system, a navigation system, and a climate control system, a driver should be able to operate these systems as well. Other than for the basic operating functions, a fine degree of control is not needed for the operating functions—they can generally be controlled by flipping a switch, as in Honda's Franz system. Moreover, voice-command control systems like that used by Samsung's Smart TV [19] could also be used. Of the basic operations requiring a fine degree of real-time control (steering, braking, and accelerating), we focus on steering, which requires the finest degree of control. The results from our research should easily be able to be transferred to braking and accelerating.

B. Steering operation requirements

Steering an automobile by moving bodily appendages should produce the same results as manually turning the wheel. Given this basic requirement, we derived four specific requirements.

- 1) *The automobile should be able to be steered within \pm about 500 degrees from the neutral position.*
 - *There should be a fine degree of steering control around the neutral position.*
 - *Steering should be quick when making a wide turn.*
- 2) *The driver should be able to keep the vehicle within the lane on both straightaways and curves of various radii at a normal driving speed.*
- 3) *The driver should be able to drive stably, and not zigzag, on straightaways.*
- 4) *The driver should be able to traverse a curve while keeping the steering wheel at a position fixed immediately before entering the curve and then exit the curve into a straightaway by gradually returning the steering wheel to the neutral position.*

C. Steering control

The steering wheel in an actual automobile can be turned about three complete revolutions from wheel lock to wheel lock ($\sim 1080^\circ$). In contrast, the movable angle of a joint angle is about $20\text{--}90^\circ$, which is much less than that of a steering wheel. Hence, it is impossible to control steering with a joint angle because it is not the same as that of a steering wheel.

We thus introduce **the non-linear steering control** and **the semi-automatic steering control**. The direct operation angle and automatic steering angle are determined, as outlined in Fig. 9, which illustrates steering control with a foot and an ankle. The driver operates using the non-linear steering control within the direct operation angle. Although Wada and Kameda used a polyline function for their steering control with a joystick, we used a non-linear function ($y = x^n$). We set $n = 3$ on the basis of our experimental results, which are described in Section VI. The steering angle increases automatically when it is beyond the direct operation angle. The rate of increase depends on the speed of

the car; the faster the car moves, the lower the rate. The driver can stop further increases in the steering angle by lifting his or her toes (about 20° for the case in Fig. 9). The driver can return the steering angle to the neutral position by lowering his or her toes. Drift error is canceled by carrying out this operation while the car is running straight.

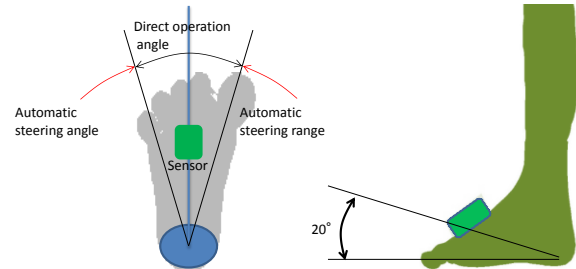


Figure 9. Example of controlling steering by foot

D. Sensor attachment and actions

We measure the car control characteristics for several actions: rolling the ankle, moving the forefinger, moving the wrist, rolling the lower arm, moving the lower arm backward and forward, and moving the upper arm backward and forward. The motions of appendages to turn a car to the right or left may differ for individuals. For example, someone may move his or her finger down to turn a car to the right, while another may move his or her finger up to turn to the right. Hence, we obtained information about different motions by individuals by administering questionnaires before measuring the car control characteristics. There were 29 participants. The results we obtained from the questionnaires are summarized in Table I. Most people chose the same action for motions that led to the right or left, such as rolling the lower arm. However, the number of people who chose alternative motions was roughly the same for motions that did not lead to the right or left such as moving his or her fingers up or down. For example, 86% of people chose rolling their right lower arm to the right to turn a car to the right. However, 52% of participants chose "up" and 48% of them chose "down" for moving their left finger up or down.

We predicted that there would be opposite relations before the questionnaires were administered between moving the right lower arm forward or backward and moving the left lower arm backward or forward, and moving the right upper arm forward or backward and moving the left upper arm backward or forward. Nevertheless, there were not extensive opposite relations, but slightly opposite relation in the results obtained from the questionnaires.

The positions of the sensors and the motions of appendages are as follows.

[Rolling ankle]

We considered using knee turning and knee movements to move gyro sensors. However, as these movements produce a narrow angle of movement, we roll the ankles. The sensor is placed on top of the foot, as shown in Fig. 9. The sensor moves when a foot are pivoted right or left on the heel.

TABLE I. RESULTS FROM QUESTIONNAIRES FOR MOTION OF TURNING CAR TO RIGHT

Left hand		Turn to right	Right hand		Turn to right
Finger	Up	15	Finger	Up	18
	Down	14		Down	11
Finger	Right	26	Finger	Forward (Right)	27
	Forward (Left)	3		Left	2
Wrist	Up	16	Wrist	Up	16
	Down	13		Down	13
Wrist	Right	24	Wrist	Right	27
	Left	5		Left	2
Lower arm	Forward	11	Lower arm	Forward	21
	Backward	18		Backward	8
Lower arm	Right	25	Lower arm	Right	28
	Left	4		Left	1
Upper arm	Forward	17	Upper arm	Forward	14
	Backward	12		Backward	15

[Moving forefinger]

There are two movements for a forefinger. The first is when the back of the hand is raised upward, the forefinger can be moved up and down, the second is when the back of the right hand is toward the right; the right forefinger can move right or left. About half the participants for the former motion chose the up direction to turn a car to the right, and the rest chose the down direction, as summarized in Table I. This means that about half of all people may make operational mistakes in the first. However, about 90% of people chose the same operation to turn a car to the right in the second. This means that most people will not make operational mistakes. Therefore, we choose the latter motion to drive a car with the forefinger. A sensor is placed on the second joint of the forefinger and is moved as shown in Fig. 10.

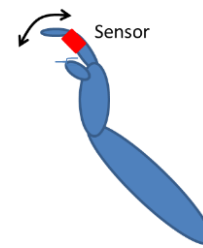


Figure 10. Moving forefinger (top view)

[Moving wrist]

There are two motions for the wrist, which are the same as those for the forefinger. We choose a motion when the back of the hand moves forward to the right and the hand moves right or left for the same reason as that for the forefinger.

The sensor is placed on the back of the hand and is moved as shown in Fig. 11.

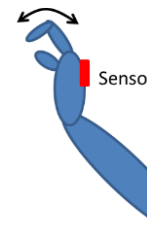


Figure 11. Moving wrist (top view)

[Moving lower arm]

We considered two motions for the lower arm. The first was moving the lower arm forward or backward, and the second was rolling the lower arm right or left. Most people will not make operational mistakes in rolling the lower arm right or left (the latter case) from the results in the questionnaires. In contrast, ~30% of people may make operational errors in the former case. However, since the ratio is less than that for the forefinger and wrist cases, we measure both their control characteristics.

The sensor is placed on the lower arm and is rolled as shown in Fig. 12.

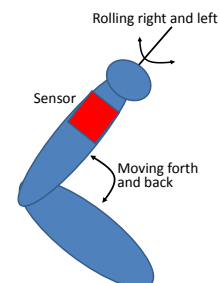


Figure 12. Rolling and moving lower arm (top view)

[Moving upper arm backward and forward]

There is not big difference between the number of participants who chose to move their right lower arm forward to turn a car to the right and the number who chose to move it backward. Therefore, this gesture is not basically suitable for the driving interface. Nevertheless, we measure it this time.

The sensor is placed above the elbow and is swung as shown in Fig. 13.

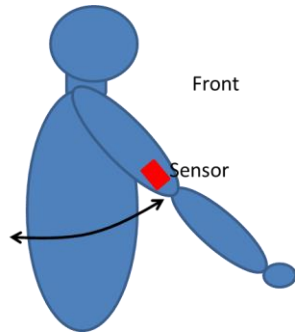


Figure 13. Moving upper arm (side view)

V. DRIVING INTERFACE EQUIPMENT

In this section, we describe various types of sensors, the type we used and its preprocessing, and the system configuration for the driving interface and its connection to a driving simulator.

A. Candidate sensors or devices

We considered five types of sensors or devices to control steering.

- Kinect sensors
- Video cameras
- Rotary encoders
- Gyro sensors
- Strain gauges

It is problematic to use Kinect sensors or video cameras because the units have to be attached to cars, and the locations for possible attachment are limited. Moreover, there must be at least 50 cm between a Kinect sensor and the gesturing appendage, which greatly limits the possible locations for attachment, as was previously mentioned.

Rotary encoders require the use of a mechanical adapter to measure the joint angle of fingers, elbows, or ankles.

Since gyro sensors are not only affected by the joint angle but also vehicle motion, they must be attached to vehicles to eliminate this effect. Moreover, gyro sensors have drift error that increases cumulatively and it is very difficult to completely remove this cumulative error. However, gyro sensors can very flexibly be attached to bodily appendages.

Strain gauges do not have drift error and are not affected by vehicle motion. Therefore, they are better suited to measuring joint angles than gyro sensors, when it is possible to attach them to joints. We plan to investigate their usefulness in future work.

B. Used sensor and its preprocessing

We used gyro sensors to evaluate gesture operations as the initial stage of our research regardless of various problems such as the influence of movements of a car to apply them to a real car. The main reasons for this were that gyro sensors are very flexible and can be attached to bodily appendages and moving joints, and the simulated car did not physically move. We used a practical 3-axis accelerometer system (ATR Promotions, WAA-010 [20]) as the sensor terminal. Not only a gyro sensor but also an accelerometer sensor, a terrestrial magnetic sensor, and a Bluetooth unit are mounted on it.

The drift phenomenon in gyro sensors is a problem for driving simulators. Angular velocity under static conditions is not zero but some other value. Example data of angular velocity and its integrated data (angle) on the WAA-006 are presented in Fig. 14. The value for angular velocity is small and varies around zero. However, since its characteristics of distribution are not normal, the value for the angle remains plus or minus for a long period. A moving average filter and 1st function adaptation are applied to reduce the drift phenomenon. The slope and the intercept of the 1st adapting function are derived from various moving averaged angular velocity data, e.g., 200 samples, under static conditions. They are automatically renewed to the latest data. Decisions under static conditions are determined from moving averaged angular velocity data that are within some threshold level. We could choose the average of the 10 largest angular velocity data under static conditions in this paper. The final output data of angular velocity are offset by the adapted 1st function. There is an example of compensated data under static conditions in Fig. 15. They remained zero under static conditions. When a gyro sensor begins to move, angular velocity data are offset by the latest adapted 1st function. Angular velocity data and their integrated data that are angle data are provided in Fig. 16 when a gyro sensor is being moved by foot.

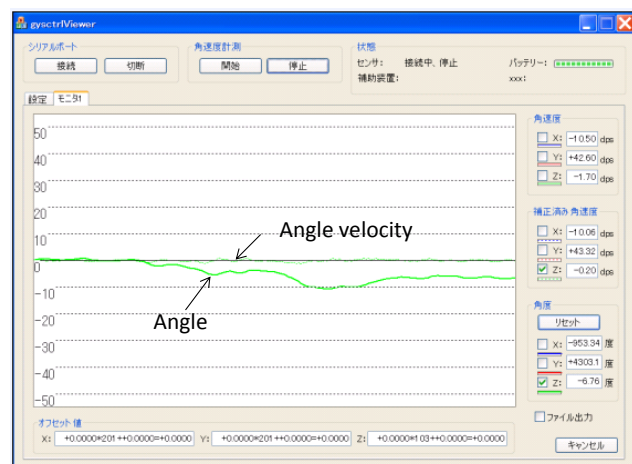


Figure 14. Uncompensated data for WAA-010 under static conditions

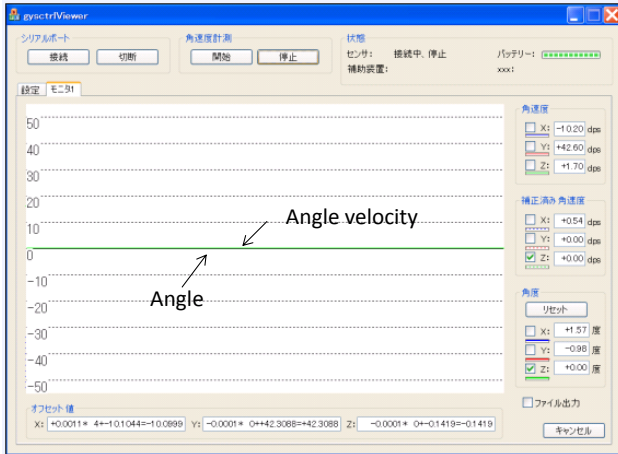


Figure 15. Compensated data of WAA-010 in static condition

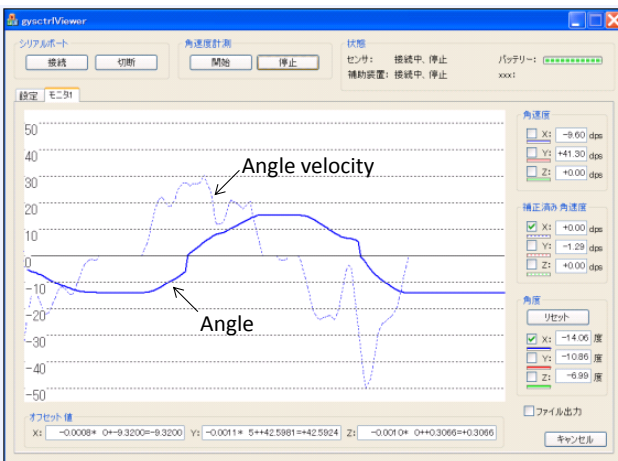


Figure 16. Angle velocity and angle data while moving WAA-010

C. Sytem configuration

We designed the driving interface we propose that will not only be used for operating a simulated car but also a real car. Therefore, the driving interface unit must be connected to a driving simulator and a real car. We designed our driving interface unit to comprise a wireless gyro sensor terminal and a PC. We developed an angle data convertor and a driving simulator and mounted them on a PC. Since the driving interface unit should be tested with an immersive driving simulator before it is applied to a real car, we also designed it to be connected to an immersive driving simulator. Therefore, the data convertor was comprised of a serial communication library, a sensor control library, an angle conversion library, and an immersive driving simulator communication library. The relationship between libraries had the layered structure shown in Fig. 17. The serial communication library provided communication functions for the Bluetooth unit. The sensor control library sent commands to control the sensor terminal WAA-010

such as the sampling rate. The angle conversion library transformed data received from the sensor terminal to a data format to enable steering control. This library contained integration that converted the angular velocity to an angle and the drift compensation function described in the previous paragraph. Since the immersive driving simulator at our university did not have a movable pedestal, this unit did not have a gyro sensor that cancelled the movements of the car. There is an example dialog box for setting the parameters in Fig. 18. It is possible to monitor output data and to set up connection parameters and compensation parameters for drift errors. The practical parameters are as follows;

Connection:

- Serial port number (COM10)
- Sampling period (5 ms)
- Average number of sampled data (5)

Drift error compensation:

- Number of data obtained for initial data (200).
- Windows size for moving average (5).
- Number of array lists for storing larger values (10).

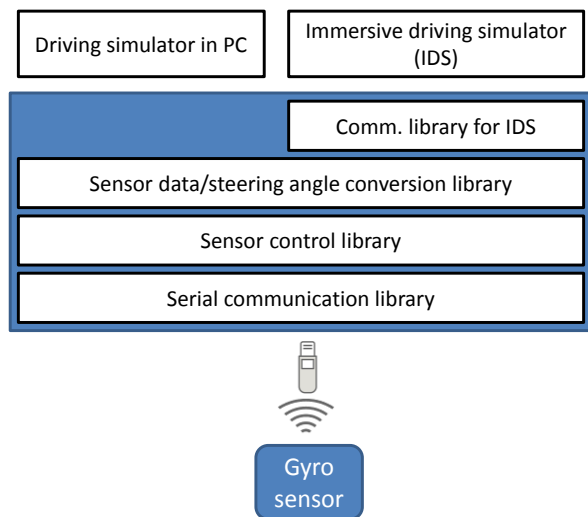


Figure 17. Configuration of the driving interface equipment

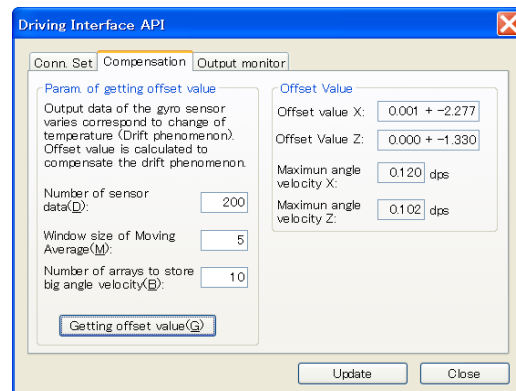


Figure 18. Dialog box for setting parameters

The values within parentheses are examples of each parameter. The offset values X and Z and the maximum angular velocities X and Z under static conditions were calculated from the above data. These data are presented on the right of the dialog box.

VI. EVALUATION

We evaluated the ability of a driver to keep within the lane and to drive stably without zigzagging on straightaways while using the proposed driving interface. Since potential users likely have difficulty moving their arms and hands, we first measured fundamental data for the foot. We then measured data for other parts of the body.

A. Evaluation issues

We calculated the ratio of lane departure (RLD) and the standard deviation of the driving gap (SDDG) to analyze performance against the 2nd and 3rd steering operation requirements described in Section IV-B;

- As can be seen from Fig. 19(a), lane departure means that one or more of the tires run on or across a lane marker line. RLD is the ratio between the distance driven and the distance during, which the car left the lane.
- As we can see from Fig. 19(b), the driving gap is the distance between the lane center and the car's center line. A value of zero means that the car is centered in the lane. SDDG is calculated using the values obtained for the car running on a straight portion of the course.

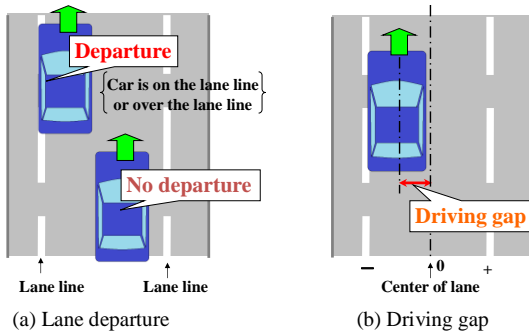


Figure 19. Lane departure and driving gap

B. Test course

As one of our ultimate aims is to help disabled people obtaining a driver's license, we use a driving route based on a typical course at a driving school (Fig. 20) to measure RLD and SDDG. It is comprised of a rectangular outer course, two crank-shaped courses, two S-shaped courses, and two parallel parking courses. The outer course is 300 x 120 m and had a corner radius of 20 m. A 3.3-m-wide driving lane runs in each of the courses.

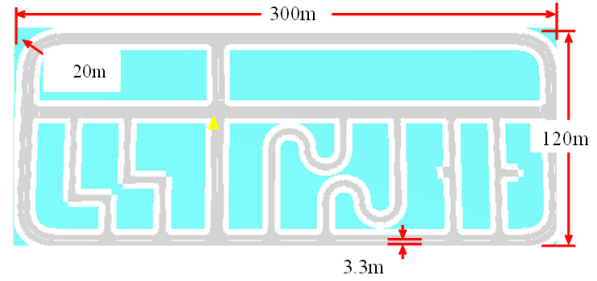


Figure 20. Driving course for evaluations

C. Results for operation by foot

Since the first objective of this research is to develop a driving interface for people with disabled arms and fingers, we focus on foot-controlled steering, as illustrated in Fig. 9.

A non-linear function ($y = x^n$) is used to control steering within the direct operation angle. We measured the position of a car on the course and calculated the RLD and SDDG for $n=1 - 4$ in $y = x^n$. We also measured and calculated the same data using a steering-wheel-type game controller for comparison. The measured and calculated data used for the non-linear function are listed in Table II for one of the four participants, who was person Y who had a great deal of experience driving a car using his foot with the proposed driving interface. These data were measured and calculated in September 2012. Since the details of the experiment by Wada and Kameda have not been published, we could not compare the precision of our control function with theirs.

TABLE II. MEASURED AND CALCULATED DATA FOR NON-LINEAR CONTROL FUNCTION FOR SKILLFUL PARTICIPANT

	$y=x$	$y=x^2$	$y=x^3$	$y=x^4$	$y=x$	Game str. wheel
Operating body part	Left feet					
DOA*	$\pm 20^\circ$				$\pm 15^\circ$	
SWA**	$\pm 180^\circ$				$\pm 30^\circ$	
Distance driven (km)	7.91	7.91	7.91	7.91	2.39	2.37
Ave. speed (km/h)	26.6	26.3	25.5	27.3	14.3	30.4
RLD (%)	0.15	0.38	0.24	0.91	9.8	0
SDDG (m)	0.21	0.24	0.27	0.29	0.15	0.11

*DOA: Direct operation angle
 **SWA: Corresponding steering wheel angle
 (Measured and calculated in Sep. 2012)

We initially thought that a driver could easily operate the car by using the semi-automatic steering control. However, the RLD and SDDG were much worse than those with the game controller when the direct operation angle (DOA) was $\pm 15^\circ$ and the corresponding steering wheel angle (SWA) was $\pm 30^\circ$. We observed that it was very difficult to drive the car using the semi-automatic steering control during typical driving maneuvers. Hence, we changed DOA to $\pm 20^\circ$ and the

corresponding SWA was $\pm 180^\circ$. It is possible to drive a car through most of the corners in normal driving within these parameters. Although neither of the two participants in this experiment negotiated the corners of the rectangular outer course smoothly at $DOA = \pm 15^\circ$ and $SWA = \pm 30^\circ$, as seen in Fig. 21, both of them could negotiate the same corners at $DOA = \pm 20^\circ$ and $SWA = \pm 180^\circ$. We concluded that controlling the car with the semi-automatic steering control was not suitable for normal driving except for parking and traversing the crank- and S-shaped courses. Detailed data traversing the crank- and S-shaped course will be given later.

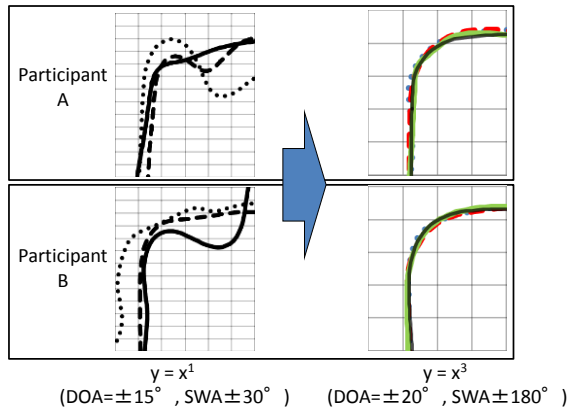
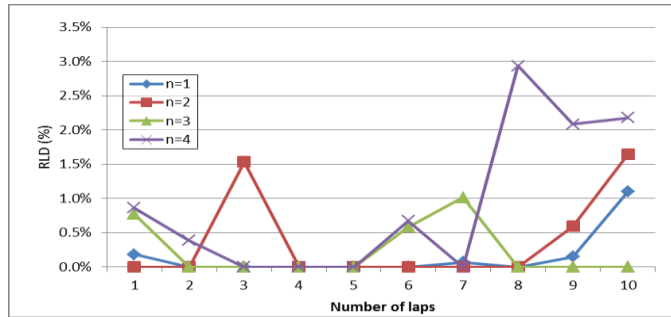
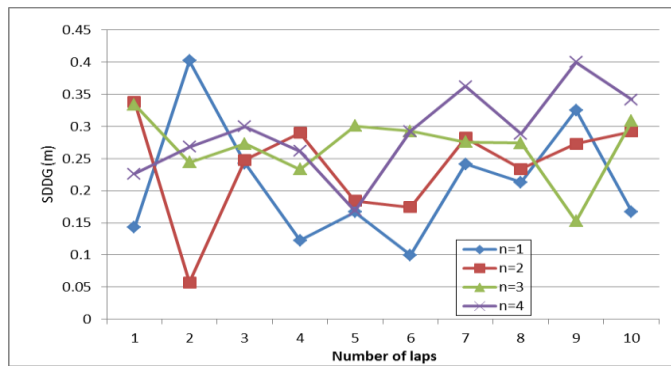


Figure 21. Cornering for participants A and B (Measured in Sep. 2012)

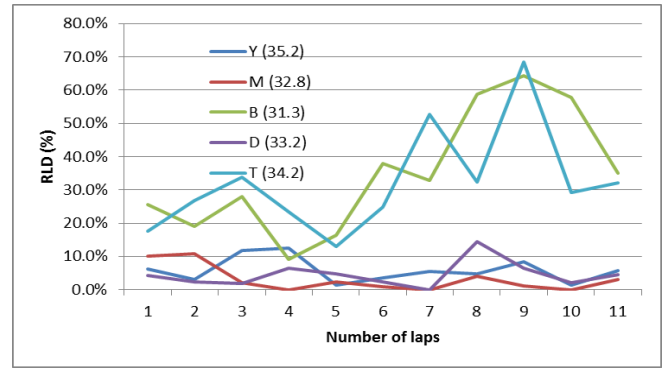


(a) RLD

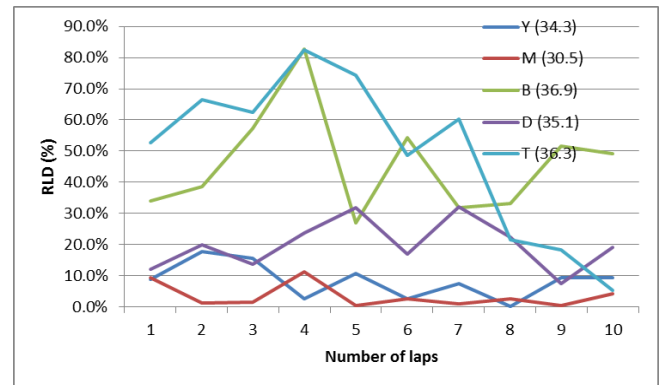


(b) SDDG

Figure 22. Car control characteristics against the number of laps (Measured in Oct. 2012), * Average speed: 26.4 km



(a) $y=x$



(b) $y=x^3$

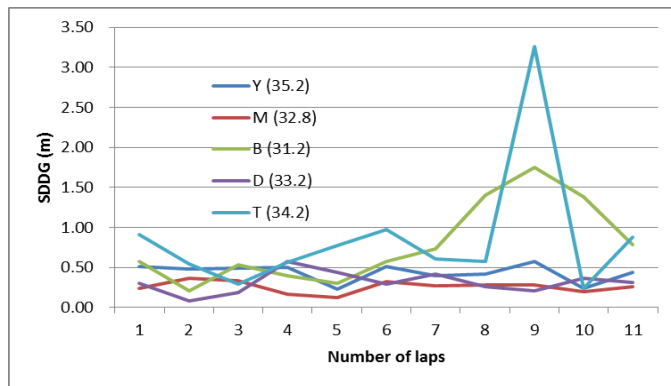
Figure 23. RLD against the number of laps (Measured in Jul. 2013)
* Average speed for each participant: written within parentheses

We considered which non-linear function was best to control the car. RLD and SDDG are the smallest for $n = 1$, as listed in Table II. However, the difference in values between $n = 1$ and $n = 3$ is negligible. Since the driving interface needs to enable a car to be driven for a long time, we measured 10 laps of the outer course for each function. The data are plotted in Fig. 22. There is not a big difference for the number of laps and the non-linear function in SDDG, but RLD is the smallest for $n=3$ during the last three laps. Since these data were measured and calculated for participant Y in Oct. 2012, we measured and calculated RLD and SDDG for four other participants in addition to participant Y at $y = x$ ($DOA = \pm 20^\circ$, $SWA = \pm 180^\circ$) and $y = x^3$ ($DOA = \pm 20^\circ$, $SWA = \pm 180^\circ$) in July 2013. The measured and calculated data for RLD and SDDG in each lap are plotted in Figs. 23 and 24. The data including those on participant Y measured and calculated in July 2013 are rather worse than those measured in Oct. 2012. Participants B and T, especially, could not drive the car well. RLD and SDDG become better in later laps at $y=x^3$, and become worse in later laps at $y=x$. B and T's data clearly reveal this tendency, and their values come close to the values of the other three participants. Although data for the other three participants have the same tendency, the changes in them are small. This tendency is the same as the data for participant Y measured and calculated in Oct. 2012. Participant Y's data in Oct. 2012 are outstanding. RLD during the last three laps is zero percent. Yet his data in Jul.

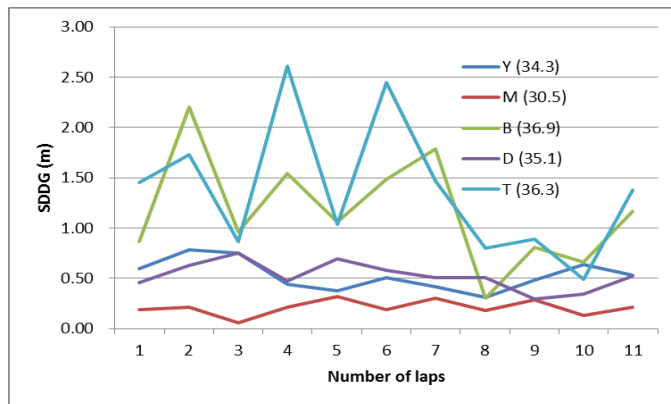
2013 are worse than his data measured and calculated 10 months earlier. Their values are roughly the same as those for participants M and D.

Although the quantity of data is insufficient, these issues suggest that most drivers can drive cars well with their feet, but they have to continue to train (i.e., drive) to retain high levels of skill. The non-linear function of $y=x^3$ may be better than $y=x$.

We calculated the RLD for the crank- and S-shaped course for four participants as well in Oct. 2012. The measured and calculated data are listed in Table III. The values are their averages. Traversing the crank- and S-shaped course is more difficult than traversing the rectangular course. The driver had to use both the non-linear and the semi-automatic steering control. Driving precision for these two courses differed greatly. As shown in Figs. 25 and 26, the precision of participant S is very close to that with the game steering wheel while that of participant C substantially diverged from it. This indicates that performance with the steering operation interface we propose should approach that with a steering wheel as the amount of practice and experience increases.



(a) $y=x$



(b) $y=x^3$

Figure 24. SDDG against the number of laps (Measured in Jul. 2013)
* Average speed for each participant: written within parentheses

TABLE III. MEASURED AND CALCULATED DATA FOR CRANK- AND S-SHAPED COURSES

	Crank-shaped course		S-shaped course	
	Game wheel	Sensor	Game wheel	Sensor
DOA	$\pm 20^\circ$			
SWA	$\pm 180^\circ$			
Cont. function	$y = x^3$ and semi-automatic steering control			
Distance driven (m)	239.7	234.6	370.8	377.4
Ave. speed (km/h)	9.7	8.3	15.0	12.9
RLD-Ave. (%)	17.2	22.9	8.9	16.8
RLD-Max. (%)	26.6	42.8	21.2	40.8
RLD-Min. (%)	6.6	8.5	0	1.2

(Measured in Oct. 2012)

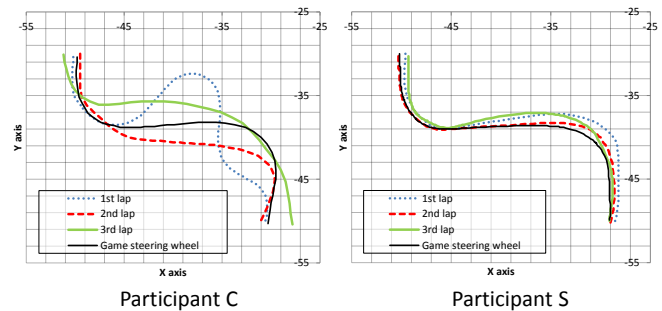


Figure 25. Crank-shaped course performance for participants C and D (Measured in Oct. 2012)

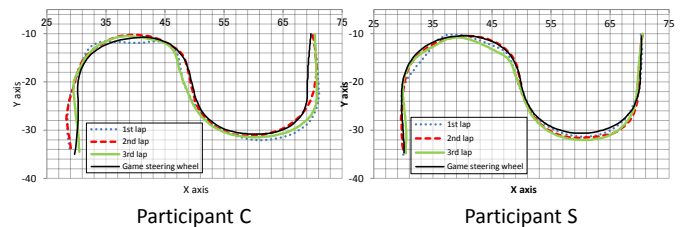


Figure 26. Precision on S-shaped course for participants C and D (Measured in Oct. 2012)

D. Results from other appendages

We measured and calculated the RLD and SDDG for steering control using the forefinger, wrist, lower arm, and upper arm in addition to the foot to examine to what extent the proposed driving interface could be applied to various types of disabilities. The data are presented in Fig. 27. There are two kinds of bars in each graph. One was measured for participant Y in Oct. 2012, and the other was measured for four participants that did not include Y in Aug. 2013. Each data was an average of driving three laps of the outer course. The movements are illustrated in Figs. 15–18. They drove three laps of the outer course.

Y's data for each appendage in Oct. 2012 are better than the data in Aug. 2013, especially Y's RLD for the foot in Oct. 2012 is very small. The reason why Y's feet data are very good is that Y trained for long periods and had a great deal of skill in controlling the car with his feet. His lengthy training and exceptional skills must have affected driving with his other appendages because their data were rather good.

There are large differences between appendages in Aug. 2013. Since this was the first time for participants who took part in the experiment to drive a simulated car with their appendages, ease of driving with each appendage for each participant clearly became apparent.

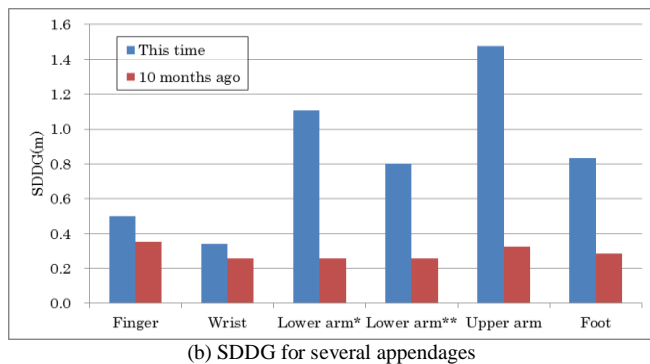
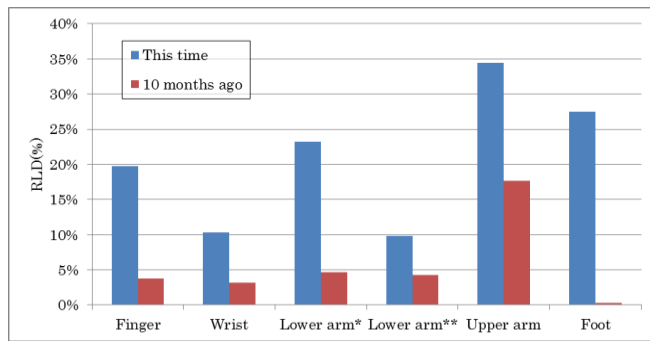


Figure 27. Car control characteristics for several appendages

- * Moving lower arm backward and forward
- ** Rolling lower arm right or left
- *** Average speed: 24.8 – 33km

The data for the upper arm is the worst because in both experiences it must have been difficult to precisely move the upper arm (and shoulder).

In any case, measured and calculated data except for the data for Y's feet in Oct. 2012 given in Fig. 27 are not sufficient to drive a car. At least, driving characteristics RLD and SDDG with each appendage must be closer to that with the game wheel. The data for participant Y measured in Oct. 2012 shows that more practice should enable users to achieve steering control closer to that with a steering wheel. Therefore, we measured driving characteristics RLD and SDDG against the training period. Moving forward or backward with the upper arm and the lower arm are not

suitable for driving a car from Table I. RLD and SDDG for both of them are not good enough in Fig. 27. We chose turning right or left with the forefinger and wrist, and rolling right or left with the lower arm. There was one participant for each gesture. The data are provided in Fig. 28. We measured the data after 30 minutes practice each day. Each data was an average of driving three laps of the outer course. The car control characteristics data improved in initial three day (90 minutes). Especially, the participant for rolling the lower arm improved in driving a car dramatically. RLD and SDDG became less than 3% and 0.3m after 5 days practice. But, SDDGs of the participant for the forefinger and the wrist on 2 September became worse than those on 31 August. The reason is that 31 August and 1 September were weekends, and the patients could not practice for two days.

Most people should be able to drive a car well by a few hours of practice regardless of irrespective of their body characteristics. But, they have to continue to train to retain high level of skills.

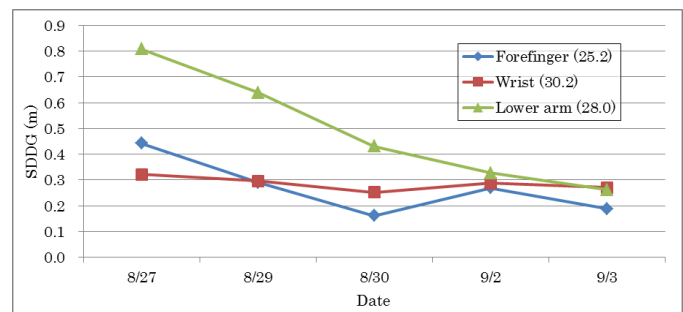
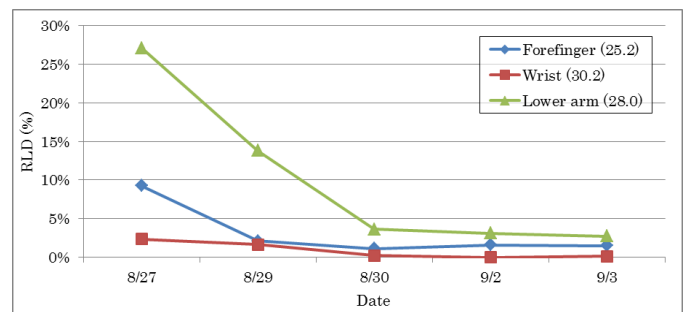


Figure 28. Car control characteristics against the number of days for practice (Measured in Aug. and Sep. 2013)

* Average speed for each participant: written within parentheses

VII. CONCLUSION

The steering operation interface we proposed for disabled people uses gesture operation. Questionnaires on gestures made with appendages indicated that gestures not leading to the right or left were not suitable for driving a car. The interface incorporated both non-linear and semi-automatic steering control. Simulated experiments using foot control and gyro sensors indicated that semi-automatic steering control was only suitable for parking and traversing crank- or s-shaped courses, and that non-linear steering control ($y=x^3$)

was better than linear steering control ($y=x$) for typical driving maneuvers. Data on worse drivers (participants in the experiment) revealed that they could not remain stable in later laps at $y=x$, but they improved in later laps at $y=x^3$. Driving operations by training the forefinger, wrist, and lower arm (rolling) were close to that achieved with a steering wheel. More practice in using the new interface should enable user to achieve steering control that is closer to that with a steering wheel.

We plan to develop a prototype of a control device using strain gauges instead of gyro sensors to avoid influencing car movements and to evaluate driving operations with it. We also plan to evaluate our proposed interface in an actual car.

ACKNOWLEDGMENT

This research has been conducted as part of the Iwate Strategic Research Foundation. We would like to express our appreciation to students in Murata-Lab, Iwate Prefectural University for taking data with our experiment.

REFERENCES

- [1] Yoshitoshi Murata, Kazuhiro Yoshida, Kazuhiro Suzuki, and Daisuke Takahashi, "Proposal of an Automobile Driving Interface Using Gesture Operation for Disabled People," IARIA ACHI 2013, March 2013.
- [2] Development of Honda's Franz System Car;
<http://world.honda.com/history/challenge/1982franzsystemcar/index.html>, December 2013.
- [3] Erico Guizzo, "How Google's Self-Driving Car Works," IEEE Spectrum, February 26, 2013.
- [4] Autonomos Labs, <http://www.autonomos.inf.fu-berlin.de/>, December 2013.
- [5] Daniel Göhring, David Latotzky, Miao Wang, and Raul Rojas, "Semi-Autonomous Car Control," Intelligent Autonomous System 12, Springer, pp. 393-408, 2013.
- [6] Joystick Driving System: allows wheelchair users to drive a car;
http://www.youtube.com/watch?v=EvMii_a7qi4, December 2013.
- [7] Masayoshi Wada and Fujio Kameda, "A joystick car drive system with seating in a wheelchair," IEEE IECON '09, pp. 2163-2168, November 2009.
- [8] FORUM8 Air Driving and RoboCar
<http://www.youtube.com/watch?v=LMr2dyfAzl0>, December 2013.
- [9] A.S.M. Mahfujur Rahman, Jamal Saboune, and Abdulmoteleb El Saddik, "Motion-path based in car gesture control of the multimedia devices," ACM DIVANet '11, Proceedings of the first ACM international symposium on Design and analysis of intelligent vehicular networks and applications, pp. 69-75, November 2011.
- [10] Tanja Döring, Dagmar Kern, Paul Marshall, Max Pfeiffer, Johannes Schöning, Volker Gruhn, and Albrecht Schmidt, "Gestural interaction on the steering wheel: reducing the visual demand," ACM CHI '11, Proceedings of the 2011 annual conference on Human factors in computing systems, pp. 483-492, May 2011.
- [11] Yoshitoshi Murata, Nobuyoshi Sato, Tsuyoshi Takayama, and Shinetsu Onodera, "A Gesture-based Remote Control for Finger Disabled People," IEEE, GCCE 2012, pp. 411-415, October 2012.
- [12] Shinya Saito, Yoshitoshi Murata, Tsuyoshi Takayama, and Nobuyoshi Sato, "An International Driving Simulator: Recognizing the Sense of a Car Body by the Simulator," Workshops in AINA 2012, W-FINA-S12.1, pp. 254-260, March 2012.
- [13] OpenGL – The Industry Standard for High Performance Graphics, <http://www.opengl.org/>, December 2013.
- [14] Simple DirectMedia Layer, <http://www.libsdl.org/>, December 2013.
- [15] The OpenGL Extension Wrangler Library, <http://glew.sourceforge.net/>, December 2013.
- [16] OpenAL Soft, <http://kcat.strangesoft.net/openal.html>, December 2013.
- [17] Masato Abe, "Automotive Vehicle Dynamics - Theory and Applications," Tokyo Denki University Press, 2008.
- [18] Giancarlo Genta, "We apply the steady gyrating movement to a car under following assumptions," World Scientific Publishing, 1997.
- [19] Samsung SMART-TV,
<http://www.samsung.com/us/2012-smart-tv/>, December 2013.
- [20] ATR Promotion WAA-010, <http://www.atr-p.com/sensor10.html>, December 2013.